

All one-loop amplitudes in $\mathcal{N} = 6$ superconformal Chern-Simons theory

Andreas Brandhuber, Gabriele Travaglini and Congkao Wen[§]

*Centre for Research in String Theory
School of Physics and Astronomy
Queen Mary University of London
Mile End Road, London E1 4NS, UK*

Abstract

We exploit a recently found connection between special triple-cut diagrams and tree-level recursive diagrams to derive a general formula capturing the multi-particle factorisation of arbitrary one-loop amplitudes in the ABJM theory. This formula contains certain anomalous contributions which are reminiscent of the so-called non-factorising contributions appearing in the factorisation of one-loop amplitudes in four-dimensional gauge theory. In the second part of the paper we derive a recursion relation for the supercoefficients of one-loop amplitudes in ABJM theory. By applying this recursion relation, any one-loop supercoefficient can be reduced to special triple-cut diagrams involving at least one four-point tree amplitude. In turn, this implies that any one-loop supercoefficient can be derived from tree-level recursive diagrams.

[§] {a.brandhuber, g.travaglini, c.wen}@qmul.ac.uk

Contents

1	Introduction	1
2	Factorisation of one-loop amplitudes	4
3	Recursion relation for supercoefficients	10
4	All one-loop amplitudes	13
4.1	Six-point amplitude at one corner	13
4.2	Eight-point amplitude at one corner	16
4.3	The general one-loop supercoefficients	17
A	On-shell solution	19

1 Introduction

In this paper we aim to study aspects of the scattering amplitudes in three-dimensional $\mathcal{N} = 6$ supersymmetric Chern-Simons (matter) theory, often referred to as ABJM theory [1]. It is a closely related cousin of $\mathcal{N} = 4$ super Yang-Mills (SYM) which provides us with a novel example of the AdS/CFT duality, the conjecture being that ABJM describes the low-energy physics of M2-branes near orbifold singularities. It also shares several properties with $\mathcal{N} = 4$ SYM although it is not maximally supersymmetric. Common features include the existence of integrable systems for the anomalous dimensions of operators [2, 3], classical integrability of the dual string theory [4–6] and Yangian symmetry of scattering amplitudes [7, 8].

Our focus will be on scattering amplitudes in ABJM theory, in particular tree-level and one-loop amplitudes and their unexpected relations. Superficially, amplitudes in ABJM and $\mathcal{N} = 4$ SYM appear to be quite similar. They can be calculated with the same tools such as on-shell recursion relations [9], (generalised) unitarity [10–12], Grassmannians [13] or twistor-string like formulae [15], and strikingly also exhibit dual conformal/Yangian symmetry [7–9, 13]. The latter appears to be a consequence of the integrable, dual string model, and its anomalous breaking [11, 14], although less studied than in $\mathcal{N} = 4$ SYM, seems to follow a similar pattern. But there are also marked differences – the gluons are non-dynamical although they have interesting, residual physical effects through their zero mode [7, 11]. Furthermore, due to the particular matter representations, only amplitudes

with even numbers of legs are non-zero and the infrared (IR) divergences are milder. In particular, tree- and one-loop amplitudes are IR finite and IR divergences appear first at two-loop order. Also the factorisation properties, which enter on-shell recursions and unitarity methods in an important way, display novel features which we will explore and exploit further below.

Compared to $\mathcal{N} = 4$ SYM, relatively little is known about amplitudes in ABJM theory, although in the recent two years the situation has improved considerably. The four-point tree amplitude [16] seeds the BCFW recursion relation [9], which allows in principle for the calculation of all tree amplitudes. The four-point amplitude at one loop was found to be vanishing in [16, 10], unlike higher-point amplitudes.¹ In particular, the six-point amplitude at one loop was explicitly computed in [11, 14, 18], while in [12] we constructed one-loop amplitudes up to ten points using a particular correspondence between special “anomalous” triple-cut diagrams and tree-level recursive diagrams. More concretely, an anomalous triple cut has a four-point amplitude as one of the tree amplitudes appearing in the cut, in which case the triple cut is in one-to-one correspondence with a BCFW recursive diagram where the two external legs of the four-point amplitude in the triple cut, say i and $i + 1$, are mapped to shifted legs \hat{i} and $\widehat{i + 1}$ in the corresponding recursive diagram. Denoting the recursive diagram evaluated on the two physically distinct pole solutions in the BCFW recursion relation by $Y^{(1)}$ and $Y^{(2)}$, the result of [12] is – schematically – that the triple-cut diagram is proportional to $Y^{(1)} - Y^{(2)}$ multiplied by a combination of sign functions (while the tree-level recursive diagram is simply $Y^{(1)} + Y^{(2)}$).

This correspondence is a close relative of the RSV formula [19], which expresses tree amplitudes in $\mathcal{N} = 4$ SYM as sums of two-mass hard coefficients, and points at a deep relations between the S-matrix of ABJM at tree and one-loop level,² which we will explore in great detail in this paper. At two loops not much is known at present, the only data point being the four-point amplitude [10, 20], whose expression surprisingly matches that of the one-loop amplitude in $\mathcal{N} = 4$ SYM, even to all orders in the expansion in the dimensional regularisation parameter ϵ [21]. Finally, Wilson loops and a possible duality to amplitudes [22–24] were studied in [25–27, 20].

The main focus of this paper is on the one-loop amplitudes in ABJM, and in particular their intriguing connections to tree amplitudes observed in [11, 14, 12]. More specifically, we will concentrate on two distinct themes: the unexpected multi-particle factorisation properties at one-loop, and a new recursion relation for one-loop supercoefficients of the ABJM amplitudes.

An important and intriguing property of the ABJM amplitudes at one loop is their infrared finiteness – a fact that can be understood from the conjectured dual conformal invariance of the theory [11] or alternatively from the impossibility to cancel infrared divergences in physical quantities at one loop because of the absence of amplitudes with an odd number of legs [12]. The finiteness of the one-loop S-matrix would naively lead to the conclusion that factorisation properties at this loop order should be trivial [28]. In particular there should be no “non-factorising contributions” of the kind found in [28] in

¹Similarities with $\mathcal{N} = 8$ SYM in three dimensions have emerged recently in [17], where it has been shown that all one-loop MHV amplitudes in this theory are vanishing.

²These similarities were firstly noticed in [11, 14] and can be understood in the six-point case from the anomalous violation of Yangian invariance.

four-dimensional gauge theory amplitudes, where the peculiarity of these contributions is that they contain kinematic invariants made of momenta from both sides of the factorisation channel, as opposed to terms appearing in the naive factorisation.³ One then faces an immediate puzzle, discussed in Section 2, concerning the factorisation of the one-loop, six-point amplitude in three-particle channels. Indeed, the six-point amplitude at one-loop is proportional to a tree-level six-point amplitude [11, 14], which has a non-trivial multi-particle factorisation in a three-particle channel. On the other hand, the vanishing of the one-loop four-point amplitude [16], onto which the six-point amplitude naively factorises, would lead to the incorrect conclusion that the one-loop six-point amplitude is finite in the factorisation limit.

We will be able to resolve this puzzle by resorting to the correspondence between three-particle cuts and BCFW tree-level diagrams [12] described earlier. As explained in detail in Section 2, we will show that in multi-particle limits some of the anomalous one-loop supercoefficients develop peculiar singularities which have a clear physical interpretation in terms of singularities of the associated BCFW recursive diagrams. As a consequence, naive factorisation has to be augmented by non-factorising contributions; in (2.29) we present the complete factorisation formula for all one-loop amplitudes in ABJM. Interestingly, our derivation of the non-factorising contributions from anomalous triple-cut diagrams (which, as recalled earlier are those containing a four-point tree amplitude as one of the amplitudes participating in the cut) is tightly linked to the peculiar role of the gluon zero-momentum mode in the tree-level four-point amplitude, that has been pointed out by [11].

In the second part of this paper we address the derivation of all one-loop supercoefficients of ABJM amplitudes, and hence of all superamplitudes at this loop order. The key tool is a very simple recursion relation, derived in Section 3, that these coefficients obey. Rather than deriving the recursion relations from factorisation, as done in [29] in four-dimensional gauge theory, we resort to a trick where, starting from a generic triple-cut diagram associated with a particular supercoefficient, we apply tree-level BCFW recursion directly to one of the tree amplitudes participating in the cut. In a generic theory, and specifically in four-dimensional Yang-Mills, this procedure gives rise to certain diagrams which cannot be cast in the form of a recursion relation (see Figure 4(b) for an example). It is a peculiarity of the ABJM amplitudes, which are non-vanishing only for an even number of legs, that such diagrams can always be avoided by appropriately choosing the legs to be shifted. As a consequence, a very simple recursion relation for supercoefficients can be derived which has the same form as the BCFW recursion for tree amplitudes. We give its final form in (3.3). By repeatedly applying this recursion relation one can evaluate all one-loop supercoefficients in terms of anomalous triple-cut diagrams, and therefore in terms of tree-level recursive diagrams. The latter are then the building blocks of all one-loop amplitudes.

The rest of the paper is structured as follows. In Section 2 we derive the multi-particle factorisation properties of one-loop amplitudes exploiting the relation between BCFW tree-level diagrams and one-loop amplitudes in ABJM found recently by the authors in [12]. In Section 3 we show that in contrast to $\mathcal{N} = 4$ SYM all integral coefficients of one-loop amplitudes in ABJM obey on-shell recursion relations if appropriate legs

³The precise definition of trivial, or naive factorisation is given in (2.1).

are shifted. Remarkably this implies that the computation of all one-loop coefficients, and hence of all one-loop amplitudes, can essentially be reduced to tree-level on-shell recursions. In Section 4 we explain in some detail how these recursion relations work in several examples and present a general, if somewhat formal, expression for the complete one-loop S-matrix. As a by-product our result establishes the Yangian invariance of all one-loop amplitudes except [11] for very specific anomalies that have their origin in sign factors appearing in the one-loop amplitudes.

2 Factorisation of one-loop amplitudes

In this section we describe multi-particle factorisation of one-loop amplitudes in ABJM theory. The case of one-loop six-point amplitudes was first discussed in [11], and in the following we will present a general factorisation formula valid for all one-loop amplitudes in ABJM. The key tool in our derivation is the correspondence found recently in [12] between particular triple-cut diagrams, where at least one of the participating amplitudes is a four-point amplitude, and tree-level recursive diagrams, as we will describe shortly.

We begin by briefly reviewing some basic facts about factorisation. The naive expectation is that amplitudes which do not have infrared divergences have trivial factorisation [28]. Since one-loop amplitudes in ABJM theory are infrared finite, one would therefore assume their factorisation to be trivial. Schematically,⁴

$$\mathcal{M}_n^{(1)} \underset{P_{1j}^2 \rightarrow 0}{\sim} \mathcal{M}_{j+1}^{(1)} \frac{1}{P_{1j}^2} \mathcal{M}_{n-j+1}^{(0)} + \mathcal{M}_{j+1}^{(0)} \frac{1}{P_{1j}^2} \mathcal{M}_{n-j+1}^{(1)}, \quad (2.1)$$

where for the sake of definiteness we focus on the channel $P_{1j} := p_1 + \dots + p_j$, and $\mathcal{M}^{(0)}$ ($\mathcal{M}^{(1)}$) denotes a tree-level (one-loop) amplitude. By definition the right-hand side of this equation contains only the singular terms and all finite terms are dropped in the limit. Similarly the expectation for tree amplitudes is to factorise as

$$\mathcal{M}_n^{(0)} \underset{P_{1j}^2 \rightarrow 0}{\sim} \mathcal{M}_{j+1}^{(0)} \frac{1}{P_{1j}^2} \mathcal{M}_{n-j+1}^{(0)}. \quad (2.2)$$

Two puzzles immediately arise with (2.1) and (2.2) when applied to ABJM amplitudes:

1. The tree-level four-point amplitude $\mathcal{M}_4^{(0)}(\bar{1}, \dots, 4)$ has a pole $1/\langle 12 \rangle$ which arises in the forward-scattering limit $p_1 + p_2 \rightarrow 0$. This is unaccounted for by (2.2), as there is no non-vanishing three-point amplitude in ABJM. However, we should emphasise that this is a rather special situation and is due to the gluon zero mode as reviewed later in this section. A generic collinear limit is of lower co-dimensionality and forces all four momenta to be collinear, in which case all four-point amplitudes vanish as expected.

2. According to (2.1), the one-loop six-point amplitude should factorise trivially in a three-particle channel, *i.e.*

$$\mathcal{M}_6^{(1)} \underset{P_{13}^2 \rightarrow 0}{\sim} \mathcal{M}_4^{(1)} \frac{1}{P_{13}^2} \mathcal{M}_4^{(0)} + \mathcal{M}_4^{(0)} \frac{1}{P_{13}^2} \mathcal{M}_4^{(1)} = 0, \quad (2.3)$$

⁴Note that in ABJM theory n must be even and j odd to have non-trivial multi-particle factorisation, since amplitudes with an odd number of legs vanish in this theory.

where the last equality follows since $\mathcal{M}_4^{(1)} = 0$ [16]. However, it is known that⁵ [18, 11, 14, 12]

$$\mathcal{M}_6^{(1)}(\bar{1}, 2, \bar{3}, 4, \bar{5}, 6) = i\pi^3 \mathcal{S}(p) \mathcal{M}_6^{(0)}(\bar{6}, 1, \bar{2}, 3, \bar{4}, 5), \quad (2.4)$$

where the prefactor $\mathcal{S}(p)$

$$\mathcal{S}(p) = \text{sgn}(\langle 1 2 \rangle) \text{sgn}(\langle 3 4 \rangle) \text{sgn}(\langle 5 6 \rangle) + \text{sgn}(\langle 2 3 \rangle) \text{sgn}(\langle 4 5 \rangle) \text{sgn}(\langle 6 1 \rangle), \quad (2.5)$$

is a special combination of sign factors defined as

$$\text{sgn}(\langle kl \rangle) := -i \frac{\langle kl \rangle}{\sqrt{-\langle kl \rangle^2 + i\varepsilon}}, \quad (2.6)$$

which is well defined for real and imaginary arguments.

Because the six-point tree amplitude on the right-hand side of (2.4) does have the nontrivial factorisation (2.2) in the three-particle channel P_{13} , it follows that (2.3), and hence (2.1), are also incomplete. Let us now proceed to identify the source of the problem and present its solution.

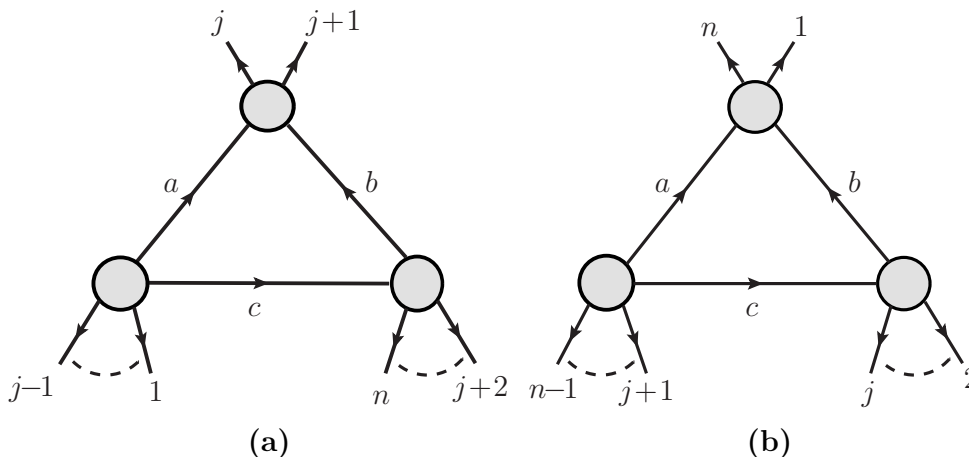


Figure 1: *The particular three-particle cut diagrams giving rise to anomalous factorisation properties of one-loop amplitudes in the $P_{1j}^2 \rightarrow 0$ limit.*

As before we focus on multi-particle factorisation of a one-loop amplitude in a kinematic channel containing an odd but otherwise arbitrary number of momenta P_{1j} . In the limit $P_{1j}^2 \rightarrow 0$ a generic triple-cut diagram contributing to the one-loop amplitude remains either finite or contributes to the naive factorisation (2.1). However, there are additional contributions from two special triple cuts, depicted in Figure 1, which also develop an unexpected simple pole of the form $1/P_{1j}^2$ in the factorisation limit. We will describe this now in detail focusing on the triple cut shown in Figure 1(a).

To begin our discussion, we recall the main result of [12], namely the fact that triple-cut diagrams containing a four-point amplitude can be associated with (and calculated in terms of the residues of) particular tree-level recursive diagrams. Specifically, the diagram in Figure 1(a) can be associated with the tree-level recursive diagram represented in Figure 2(a). The main idea can be conveyed schematically as follows.

⁵We follow the notation and conventions of Section 2 and Appendix A of [12] for the ABJM superamplitudes and the three-dimensional spinor helicity formalism, respectively.

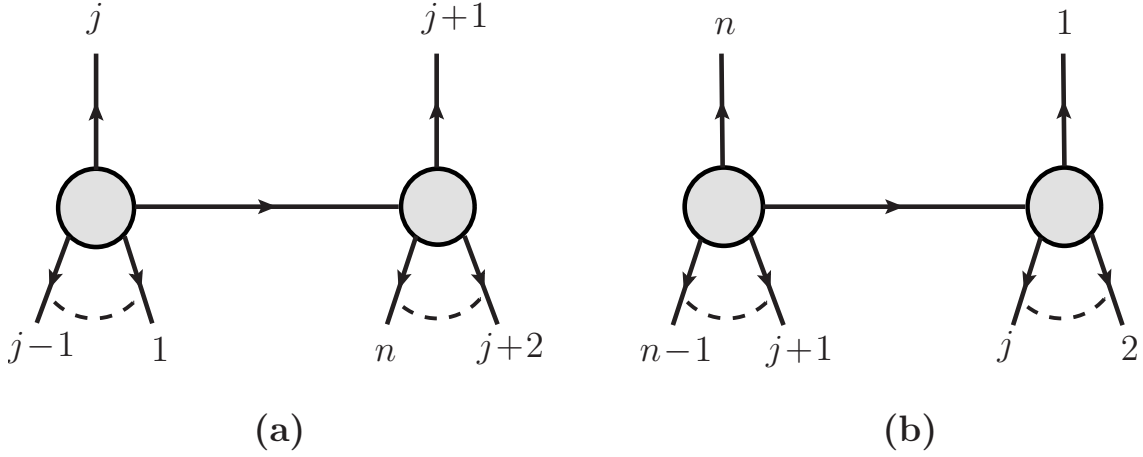


Figure 2: The two tree-level factorisation diagrams associated to the triple-cut diagrams in Figure 1.

The supercoefficient associated with the triple cut of Figure 1(a) is equivalent to the recursive diagram shown in Figure 2(a). The crucial observation is that in the factorisation limit $P_{1j}^2 \rightarrow 0$ the usual shifts of the external momenta implied in the BCFW diagram are removed, since the internal propagator in Figure 2(a) goes on shell as $P_{1j}^2 \rightarrow 0$. Therefore, in this limit the supercoefficient can be written schematically as

$$\mathcal{C}_{jj+1;n} \underset{P_{1j}^2 \rightarrow 0}{\sim} \mathcal{M}_L^{(0)} \frac{1}{P_{1j}^2} \mathcal{M}_R^{(0)}. \quad (2.7)$$

The triple-cut diagram in Figure 1(b) gives a similar contribution. The final result has the form

$$\mathcal{M}_L^{(0)} \frac{\mathcal{F}}{P_{1j}^2} \mathcal{M}_R^{(0)}, \quad (2.8)$$

where the coefficient function \mathcal{F} will be determined below. This anomalous factorisation term has the structure of a product of two tree-level amplitudes multiplied by a propagator and the coefficient function \mathcal{F} . Importantly, this function depends on kinematic invariants with external momenta from both sides of the factorisation channel, and hence is less universal than the naive factorisation contributions. We note that (2.8) has the same form of the so-called “non-factorising terms” discussed in [28] in the context of four-dimensional gauge theories.

Let us now fill in the details omitted in the previous qualitative discussion, and derive the general formula capturing the factorisation of all one-loop amplitudes in ABJM. In order to do so, we briefly review the results of [12], focusing again on the triple-cut diagram of Figure 1(a). It was found in [12] that the cut momenta $(l_a)_{\alpha\beta} := \hat{\lambda}_{a;\alpha} \hat{\lambda}_{a;\beta}$ and $(l_b)_{\alpha\beta} := \hat{\lambda}_{b;\alpha} \hat{\lambda}_{b;\beta}$ of the triple-cut diagram of Figure 1(a) can be expressed in terms of the spinors $\hat{\lambda}_a$ and $\hat{\lambda}_b$ defined as

$$\begin{pmatrix} \hat{\lambda}_a \\ \hat{\lambda}_b \end{pmatrix} = R(z) \begin{pmatrix} \lambda_j \\ \lambda_{j+1} \end{pmatrix}, \quad (2.9)$$

where $R(z)$ is a rotation matrix, parameterised as

$$R(z) = \begin{pmatrix} \frac{1}{2}(z + z^{-1}) & -\frac{1}{2i}(z - z^{-1}) \\ \frac{1}{2i}(z - z^{-1}) & \frac{1}{2}(z + z^{-1}) \end{pmatrix}. \quad (2.10)$$

The shift parameter z , which is the analogue of the deformation parameter z of four-dimensional BCFW recursion relations, is fixed by solving the remaining on-shell condition

$$l_c^2 = (l_a + K_1)^2 = 0, \quad (2.11)$$

with $K_1 = P_{1j-1}$. It was shown in [9] and also in Section 3 of [12] that this condition can be put in the form

$$az^{-2} + b + cz^2 = 0, \quad (2.12)$$

with

$$a = 2(\tilde{q} \cdot K_1), \quad b = -K_1 \cdot K_2, \quad c = 2(q \cdot K_1), \quad (2.13)$$

where

$$q^{\alpha\beta} := \frac{1}{4}(\lambda_j + i\lambda_{j+1})^\alpha(\lambda_j + i\lambda_{j+1})^\beta, \quad \tilde{q}^{\alpha\beta} := \frac{1}{4}(\lambda_j - i\lambda_{j+1})^\alpha(\lambda_j - i\lambda_{j+1})^\beta, \quad (2.14)$$

and $K_2 := P_{j+2n}$. In this notation

$$l_a := \hat{\lambda}_a \hat{\lambda}_a = z^2 q + z^{-2} \tilde{q} + \frac{1}{2}(p_j + p_{j+1}), \quad (2.15)$$

and the explicit solutions are

$$z_1^2 = \frac{K_1 \cdot K_2 + \sqrt{K_1^2 K_2^2}}{4(q \cdot K_1)}, \quad z_2^2 = \frac{K_1 \cdot K_2 - \sqrt{K_1^2 K_2^2}}{4(q \cdot K_1)}. \quad (2.16)$$

The supercoefficient in Figure 1(a) is then given by [12]

$$\mathcal{C}_{jj+1;n} = -\langle jj+1 \rangle \sqrt{K_1^2 K_2^2} \left(Y_{jj+1;n}^{(1)} - Y_{jj+1;n}^{(2)} \right), \quad (2.17)$$

where $Y_{jj+1;n}^{(a)}$, $a = 1, 2$ is the result of the recursive diagram in Figure 2(a) evaluated on the solution $z = z_a$, *i.e.* [9]

$$Y_{jj+1;n}^{(1)} = \int d^3 \eta_c \frac{H(z_1, z_2)}{P_{1j}^2} \left[\mathcal{M}_R(\widehat{j+2}, \dots, n, -\bar{c}, \widehat{j+1}) \mathcal{M}_L(\bar{1}, \dots, j-1, \bar{j}, c) \right]_{z=z_1}, \quad (2.18)$$

with $Y_{jj+1;n}^{(2)} = [Y_{jj+1;n}^{(1)}]_{z_1 \leftrightarrow z_2}$, and the function H is defined as

$$H(z_1, z_2) := \frac{z_1(z_2^2 - 1)}{z_1^2 - z_2^2}. \quad (2.19)$$

Rewriting the off-shell momenta K_1 and K_2 in three-dimensional spinor notation as

$$K_{1ab} := \xi_{(a} \mu_{b)}, \quad K_{2ab} := \xi'_{(a} \mu'_{b)}, \quad (2.20)$$

with $K_1^2 K_2^2 = (1/16) \langle \xi \mu \rangle^2 \langle \xi' \mu' \rangle^2$, we can re-express (2.17) as follows:

$$\mathcal{C}_{jj+1;n} = \frac{\langle jj+1 \rangle}{4} \langle \xi \mu \rangle \langle \xi' \mu' \rangle \left(Y_{jj+1;n}^{(1)} - Y_{jj+1;n}^{(2)} \right). \quad (2.21)$$

We are interested in finding the behaviour of the triple-cut diagram of Figure 1(a) in the multi-particle factorisation limit $P_{1j}^2 \rightarrow 0$. In this limit, the coefficients a, b, c introduced in (2.13) satisfy the relation $a + b + c \rightarrow 0$, from which one infers that

$$z_2^2 \rightarrow 1. \quad (2.22)$$

Curiously, the specific limiting value of z_1 will be immaterial in the following discussion.

Next we take the factorisation limit $P_{1j}^2 \rightarrow 0$ on (2.21). In this limit

$$H(z_1, z_2) \rightarrow 0, \quad H(z_2, z_1) \rightarrow -1, \quad (2.23)$$

hence only the second term in (2.21) survives:

$$\mathcal{C}_{jj+1;n} \xrightarrow{P_{1j}^2 \rightarrow 0} \frac{\langle jj+1 \rangle}{4} \langle \xi \mu \rangle \langle \xi' \mu' \rangle \int d^3 \eta_c \frac{1}{P_{1j}^2} \left[\mathcal{M}_R^{(0)}(\bar{j}+2, \dots, n, -\bar{c}, j+1) \mathcal{M}_L^{(0)}(\bar{1}, \dots, j-1, \bar{j}, c) \right], \quad (2.24)$$

where we note that we were able to remove the BCFW shifts from legs j and $j+1$, as these are turned off when $z \rightarrow 1$.

Finally, the contribution to the factorisation of the amplitude is obtained by multiplying (2.24) with the corresponding three-mass triangle function

$$\begin{aligned} \mathcal{I}^{3m}(K_1, K_2, K_3) &:= \int d^3 l \frac{1}{(l^2 + i\varepsilon)((l + K_1)^2 + i\varepsilon)((l + K_1 + K_2)^2 + i\varepsilon)} \\ &= \frac{-i \pi^3}{\sqrt{-(K_1^2 + i\varepsilon)} \sqrt{-(K_2^2 + i\varepsilon)} \sqrt{-(K_3^2 + i\varepsilon)}}, \end{aligned} \quad (2.25)$$

with $K_3 = p_j + p_{j+1}$ in the case at hand. Doing so we arrive at the result

$$\begin{aligned} &\mathcal{C}_{jj+1;n} \mathcal{I}(P_{j+2n}, P_{1j-1}, P_{jj+1}) \xrightarrow{P_{1j}^2 \rightarrow 0} \\ &-i \frac{\pi^3}{4} \frac{\langle jj+1 \rangle}{\sqrt{-(P_{jj+1}^2 + i\varepsilon)}} \frac{\langle \xi \mu \rangle}{\sqrt{-(P_{1j-1}^2 + i\varepsilon)}} \frac{\langle \xi' \mu' \rangle}{\sqrt{-(P_{j+2n}^2 + i\varepsilon)}} \\ &\times \int d^3 \eta_c \frac{1}{P_{1j}^2} \left[\mathcal{M}_R(\bar{j}+2, \dots, n, -\bar{c}, j+1) \mathcal{M}_L(\bar{1}, \dots, j-1, \bar{j}, c) \right], \end{aligned} \quad (2.26)$$

where we set $(P_{1j-1})_{\alpha\beta} := \xi_{(\alpha} \mu_{\beta)}$, and $(P_{j+2n})_{\alpha\beta} := \xi'_{(\alpha} \mu'_{\beta)}$.

There is another contribution to add, namely that of Figure 1(b). This can be associated with the recursive diagram in Figure 2(b) and is given by

$$\begin{aligned} &\mathcal{C}_{n1;j} \mathcal{I}(P_{n1}, P_{j+1n-1}, P_{2j}) \xrightarrow{P_{1j}^2 \rightarrow 0} \\ &-i \frac{\pi^3}{4} \frac{\langle n1 \rangle}{\sqrt{-(P_{n1}^2 + i\varepsilon)}} \frac{\langle \tilde{\xi} \tilde{\mu} \rangle}{\sqrt{-(P_{2j}^2 + i\varepsilon)}} \frac{\langle \tilde{\xi}' \tilde{\mu}' \rangle}{\sqrt{-(P_{j+1n-1}^2 + i\varepsilon)}} \end{aligned}$$

$$\times \int d^3 \eta_c \frac{1}{P_{1j}^2} \left[\mathcal{M}_R(\overline{j+2}, \dots, n, -\bar{c}, j+1) \mathcal{M}_L(\bar{1}, \dots, j-1, \bar{j}, c) \right] \quad (2.27)$$

with $(P_{2j})_{\alpha\beta} := \tilde{\xi}_{(\alpha} \tilde{\mu}_{\beta)}$ and $(P_{j+1n-1})_{\alpha\beta} := \tilde{\xi}'_{(\alpha} \tilde{\mu}'_{\beta)}$. Hence the total anomalous factorisation term is obtained by summing (2.26) and (2.27), and reads

$$\mathcal{F} \times \int d^3 \eta_c \frac{1}{P_{1j}^2} \left[\mathcal{M}_R^{(0)}(\overline{j+2}, \dots, n, -\bar{c}, j+1) \mathcal{M}_L^{(0)}(\bar{1}, \dots, j-1, \bar{j}, c) \right],$$

where

$$\begin{aligned} \mathcal{F} = & -i \frac{\pi^3}{4} \left[\frac{\langle jj+1 \rangle}{\sqrt{-(P_{jj+1}^2 + i\varepsilon)}} \frac{\langle \xi \mu \rangle}{\sqrt{-(P_{1j-1}^2 + i\varepsilon)}} \frac{\langle \xi' \mu' \rangle}{\sqrt{-(P_{j+2n}^2 + i\varepsilon)}} + \right. \\ & \left. + \frac{\langle n1 \rangle}{\sqrt{-(P_{n1}^2 + i\varepsilon)}} \frac{\langle \tilde{\xi} \tilde{\mu} \rangle}{\sqrt{-(P_{2j}^2 + i\varepsilon)}} \frac{\langle \tilde{\xi}' \tilde{\mu}' \rangle}{\sqrt{-(P_{j+1n-1}^2 + i\varepsilon)}} \right]. \end{aligned} \quad (2.28)$$

In summary, the complete factorisation formula for one-loop amplitudes in ABJM theory is given by⁶

$$\begin{aligned} \mathcal{M}_n^{(1)} \xrightarrow{P_{1j}^2 \rightarrow 0} & \mathcal{M}_{j+1}^{(1)} \frac{1}{P_{1j}^2} \mathcal{M}_{n-j+1}^{(0)} + \mathcal{M}_{j+1}^{(0)} \frac{1}{P_{1j}^2} \mathcal{M}_{n-j+1}^{(1)} \\ & + \mathcal{M}_{j+1}^{(0)} \frac{\mathcal{F}}{P_{1j}^2} \mathcal{M}_{n-j+1}^{(0)}, \end{aligned} \quad (2.29)$$

where \mathcal{F} is given by (2.28). The first line of (2.29) captures the naive factorisation, while the second line represents the non-factorising term.

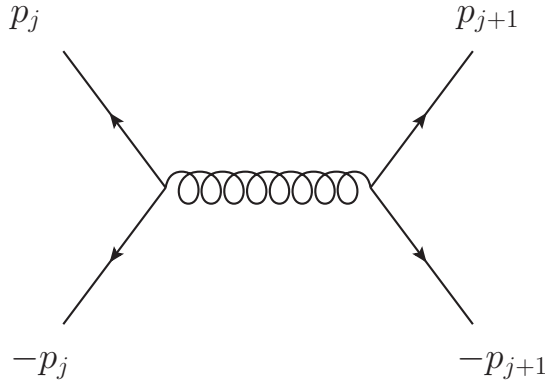


Figure 3: *The dominant Feynman diagram contributing to the forward-scattering limit of the four point-amplitude $\mathcal{M}_4^{(0)}(-p_j, p_j, p_{j+1}, -p_{j+1})$. The exchanged gluon has vanishing momentum.*

Let us briefly pause here to discuss the subtle role played by the gluon zero-modes. It was suggested in [11] that the non-factorising terms are associated with the propagation of

⁶In the following formula, integration over η_c is understood.

a gluon zero-momentum mode. This is precisely what emerges from the analysis presented in this section. Focusing again on the triple cut in Figure 1(a), we observe that as $P_{1j}^2 \rightarrow 0$, the cut momenta l_a and l_b tend to the limiting values

$$l_a \rightarrow p_j, \quad l_b \rightarrow p_{j+1}, \quad \text{as } P_{1j}^2 \rightarrow 0. \quad (2.30)$$

This is nothing but the well-known forward-scattering limit of the four-point amplitude $\mathcal{M}^{(0)}(-l_a, -l_b, p_j, p_{j+1})$. In this limit the amplitude is singular [7], with the singularity coming from the particular Feynman diagram drawn in Figure 3, where a pair of (unscattered) particles exchanges a gluon with zero three-momentum.

We conclude this section by applying our general result on one-loop factorisation to the simple example of the one-loop six-point amplitude. More concretely, we consider the multi-particle factorisation channel $P_{13}^2 \rightarrow 0$. As discussed earlier, there is no one-loop four-point amplitude in ABJM theory, hence the first line of (2.29) vanishes. In this case there are two different three-particle cut diagrams contributing to the non-factorising terms, where the external legs are grouped as (61), (23), (45) and (34), (56), (21). The non-factorising term \mathcal{F} given in (2.28) is easily found to be

$$\mathcal{F}_{P_{13}^2} = \pi^3 \left[\text{sgn}(\langle 61 \rangle) \text{sgn}(\langle 23 \rangle) \text{sgn}(\langle 45 \rangle) + \text{sgn}(\langle 34 \rangle) \text{sgn}(\langle 56 \rangle) \text{sgn}(\langle 12 \rangle) \right], \quad (2.31)$$

where we have used the relations $\langle \xi \mu \rangle = -2i \langle 12 \rangle$, $\langle \xi' \mu' \rangle = -2i \langle 56 \rangle$, $\langle \tilde{\xi} \tilde{\mu} \rangle = -2i \langle 45 \rangle$, and $\langle \tilde{\xi}' \tilde{\mu}' \rangle = -2i \langle 23 \rangle$, and $\text{sgn}(\langle ij \rangle)$ is defined in (2.6).

As a final comment we would like to add that it would be tempting to construct a BCFW style recursion for one-loop amplitudes in ABJM theory based on our complete understanding of factorisation (2.29). We have not attempted this here and leave this for future studies. Note that in the next section we will follow a slightly different route and introduce recursion relations for integral coefficients which allow us to construct at least in principle the complete one-loop S-matrix of ABJM theory.

3 Recursion relation for supercoefficients

The coefficients of L -loop amplitudes are rational functions just as tree-level amplitudes, and hence it is natural to consider on-shell recursion relations for them. This idea was applied for the first time to one-loop amplitudes in four-dimensional gauge theory in [29]. However, one has to face two potential problems: firstly, individual integral coefficients may have spurious poles which have to cancel in the complete amplitude; and furthermore, it is not known a priori if the coefficients have the desired large- z behaviour under BCFW shifts. However, in [29] a set of criteria has been derived under which recursion relations can be applied directly to coefficients.

An elegant way to avoid all the above mentioned problems in one stroke is to use BCFW shifts of two legs that sit at the same corner of a cut loop diagram [29]. This effectively relates the recursion relation for a coefficient to the recursion relation for a tree amplitude (which we fully understand) which appears as one factor in the expression for the coefficient obtained from generalised unitarity. Hence the knowledge of tree-level

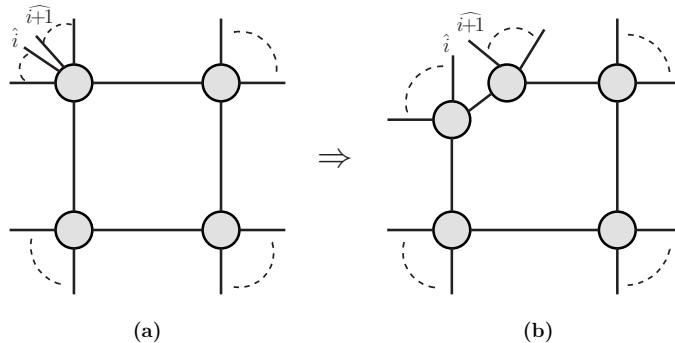


Figure 4: In (b) we show a possible diagram which may appear when applying the BCFW recursion relation to the top left tree amplitude in the quadruple cut shown in (a). Such a situation cannot be avoided in general in $\mathcal{N} = 4$ SYM, and the diagram in (b) cannot be described using recursion relations for supercoefficients. \hat{i} and $\widehat{i+1}$ denote the shifted legs.

amplitudes allows us to determine the poles as well as the large- z behaviour. However some more care is needed, since the recursion relation will in general include diagrams such as that in Figure 4(b), where the propagator of the BCFW diagram is part of the (cut) loop diagram. In this case z dependence would enter the loop integration, lead to z -dependent spurious singularities, and destroy our attempt to construct an on-shell recursion relation for coefficients. This is exactly the reason why there is no simple BCFW recursion relation for general supercoefficients in $\mathcal{N} = 4$ SYM. On the other hand, if we are able to avoid channels of the type depicted in Figure 4(b), then the recursion relation for coefficients follows immediately from that for tree-level amplitudes.

As we will now demonstrate ABJM theory does have such recursion relations for all one-loop supercoefficients.⁷ The crucial property of ABJM that makes this possible is that all amplitudes with an odd number of particles vanish. This immediately implies that a recursive diagram such as that in Figure 4(b) can always be avoided by choosing appropriate locations for the shifted legs (labelled by \hat{i} and $\widehat{i+1}$ in Figure 4). Let us consider the concrete example in Figure 5, where the supercoefficient is given by the triple cut averaged over the two inequivalent solutions $l_{a,s}$, $s = 1, 2$ for the cut momentum l_a ,

$$\begin{aligned} \mathcal{C}_{n;1,2,\dots,m;i} &= \frac{1}{2} \sum_{s=1}^2 \int d^3\eta_a d^3\eta_b d^3\eta_c \mathcal{M}^{(0)}(\bar{1}, \dots, m, -\bar{b}_s, -a_s) \\ &\times \mathcal{M}^{(0)}(\overline{m+1}, \dots, i, -\bar{c}_s, b_s) \mathcal{M}^{(0)}(\widehat{i+1}, \dots, n, \bar{a}_s, c_s), \end{aligned} \quad (3.1)$$

and $a_s := (\lambda_{l_{a,s}}, \eta_a)$, with similar definitions for b_s and c_s . From the above analysis, shifting 1 and 2 is one possible valid BCFW shift⁸, as indicated in Figure 5. We can then apply the BCFW tree-level recursion relation, which only affects the tree-amplitude in

⁷The authors of [29] were able to find valid recursion relations for bubble and triangle coefficients in four-dimensional gauge theories.

⁸In fact shifting any i and $i+1$ would also work when i is odd.

the top corner of the triple-cut diagram of Figure 5, and obtain

$$\begin{aligned}
\mathcal{C}_{n;1,\dots,m;i} &:= \mathcal{C}(\bar{1}, 2, \dots, m; \overline{m+1}, \dots, i; \overline{i+1}, \dots, n) \\
&= \frac{1}{2} \sum_{s=1}^2 \int d^3\eta_a d^3\eta_b d^3\eta_c d^3\eta_{\hat{P}} \\
&\quad \sum_k \frac{H(z_1, z_2)}{p_f^2} \left[\mathcal{M}^{(0)}(\bar{3}, \dots, k, -\bar{\hat{P}}, \hat{2}) \mathcal{M}^{(0)}(\overline{k+1}, \dots, -a_s, -\bar{b}_s, \bar{1}, \hat{P}) \right]_{z=z_1} \\
&\quad \times \mathcal{M}^{(0)}(\overline{m+1}, \dots, i, -\bar{c}_s, b_s) \mathcal{M}^{(0)}(\overline{i+1}, \dots, n, \bar{a}_s, c_s) \\
&\quad + (z_1 \leftrightarrow z_2), \tag{3.2}
\end{aligned}$$

where $z_{1,2}$ denote the position of the poles in the BCFW recursion relation for the tree amplitude $\mathcal{M}^{(0)}(\bar{1}, \dots, m, -\bar{b}_s, -a_s)$. These are obtained from (2.16) with $K_1 = p_{k+1} + \dots + p_n$, and $K_2 = p_3 + \dots + p_k$, since $-(p_a + p_b) = p_{m+1} + \dots + p_n$. Note that $z_{1,2}$ and, hence, \hat{P} are independent of the cut loop momenta. We should stress that this point is crucial since it implies that the BCFW shifts do not affect the cut momenta of the triple cut. Therefore, we can now rewrite (3.2) as a recursion relation for supercoefficients directly:

$$\begin{aligned}
\mathcal{C}_{n;1,\dots,m;i} &= \sum_k (-)^{\frac{m+k}{2}+1} \int d^3\eta_{\hat{P}} \frac{H(z_1, z_2)}{p_f^2} \left[\mathcal{M}^{(0)}(\bar{3}, \dots, k, -\bar{\hat{P}}, \hat{2}) \right. \\
&\quad \left. \times \mathcal{C}(\bar{1}, \hat{P}, \overline{k+1}, \dots, m; \overline{m+1}, \dots, i; \overline{i+1}, \dots, n) \right]_{z=z_1} \\
&\quad + (z_1 \leftrightarrow z_2), \tag{3.3}
\end{aligned}$$

where the extra sign factor $(-)^{\frac{m+k}{2}+1}$ arises from the behaviour of the amplitude under cyclic shifts of its arguments,

$$\mathcal{M}^{(0)}(\overline{k+1}, \dots, -a, -\bar{b}, \bar{1}, \hat{P}) = (-)^{\frac{m+k}{2}+1} \mathcal{M}^{(0)}(\bar{1}, \hat{P}, \overline{k+1}, \dots, -a, -\bar{b}). \tag{3.4}$$

The reason for this is that we have defined the supercoefficients in such a way that the two cut legs of every tree-level amplitude appear as the last two arguments, as in (3.1). Note that this is necessary in order to fix any sign ambiguities.

Eq. (3.3) is the main result of this section. Since in the following sections we will make use of shifts applied to legs $m-1$ and m , we present here the corresponding recursion relation as well,

$$\begin{aligned}
\mathcal{C}_{n;1,\dots,m;i} &= \sum_k (-)^{\frac{km}{4}+1} \int d^3\eta_{\hat{P}} \frac{H(z_1, z_2)}{p_f^2} \left[\mathcal{M}^{(0)}(\bar{k}, \dots, \overline{m-1}, \hat{P}) \right. \\
&\quad \left. \times \mathcal{C}(\bar{1}, \dots, k-1, -\bar{\hat{P}}, \hat{m}; \overline{m+1}, \dots, i; \overline{i+1}, \dots, n) \right]_{z_1} + (z_1 \leftrightarrow z_2). \tag{3.5}
\end{aligned}$$

A key property of the BCFW recursion is that it relates all higher-point amplitudes to the smallest amplitudes in a given theory, which in the case of ABJM can be packaged neatly

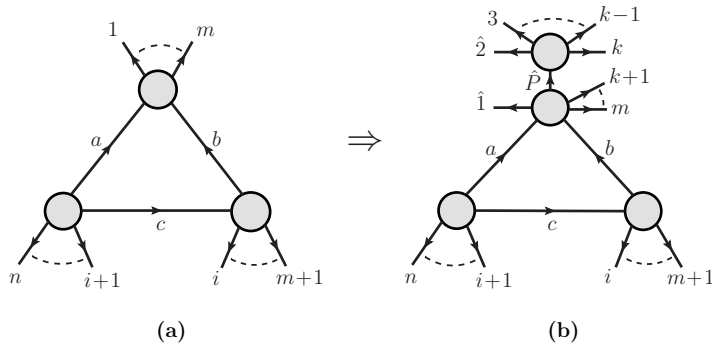


Figure 5: In (b) we show a recursive diagram for the supercoefficient $\mathcal{C}_{n;1,\dots,m;i}$ of a one-loop amplitude in ABJM, calculated by the triple cut in (a).

into the four-point superamplitude. Therefore we can recursively reduce any corner (of a triple cut) with a higher-point amplitude to a four-point amplitude. Furthermore, it was shown recently by the present authors that every triple cut involving at least one four-point (super)amplitude itself is in one-to-one correspondence with a tree-level recursive diagram [12]. Combining these results, we infer that all triple cuts, and hence all one-loop triangle coefficients in ABJM, are effectively related by tree-level recursion relations. This close relationship between tree-level recursion relations and one-loop amplitudes in ABJM will be explored and made more precise in the following sections. We also note that this connection makes the Yangian invariance [9, 7] of one-loop amplitudes in ABJM manifest up to the anomalies discussed in [11].

4 All one-loop amplitudes

In this section we illustrate with concrete examples how supercoefficients of one-loop amplitudes in ABJM can be calculated efficiently using the recursion relation formulated in the previous section. In particular all supercoefficients can be related to special ones where one of the tree amplitudes in the triple-cut diagram is a four-point amplitude. Since such coefficients can be calculated from an associated tree-level recursive diagram [12], this implies that the calculation of all one-loop supercoefficients can be reduced to that of tree recursive diagrams. The supercoefficients with a four-point amplitude in a corner are therefore the seeds for generic supercoefficients.

4.1 Six-point amplitude at one corner

We start with the simplest supercoefficient, when one corner of the associated triple-cut diagram is a six-point tree-level amplitude, as shown in Figure 6. In this case the supercoefficient has the form

$$\mathcal{C}_{n;1234;i} = \frac{1}{2} \sum_{s=1}^2 \int d^3\eta_a d^3\eta_b d^3\eta_c$$

$$\mathcal{M}^{(0)}(\bar{1}, 2, \bar{3}, 4, -\bar{b}_s, -a_s) \mathcal{M}^{(0)}(\bar{5}, \dots, i, -\bar{c}_s, b_s) \mathcal{M}^{(0)}(\overline{i+1}, \dots, n, \bar{a}_s, c_s). \quad (4.1)$$

As discussed in Section 3, this supercoefficient can be expressed with a recursion relation with shifts applied to legs 1 and 2 as

$$\mathcal{C}_{n;1234;i} = - \left[\mathcal{M}^{(0)}(\bar{3}, 4, -\hat{\bar{P}}, \hat{2}) \circ \mathcal{C}_{n-2;\hat{1}\hat{P};i} \right]_{z=z_1} + (z_1 \leftrightarrow z_2), \quad (4.2)$$

where we have introduced the compact notation

$$\left[\mathcal{A} \circ \mathcal{B} \right]_{z=z_1} \rightarrow \int d^3 \eta_{\hat{P}} \frac{H(z_1, z_2)}{p_f^2} \left[\mathcal{A} \mathcal{B} \right]_{z=z_1}. \quad (4.3)$$

The supercoefficient $\mathcal{C}_{n-2;\hat{1}\hat{P};i}$ is obtained from a triple-cut diagram where one of the

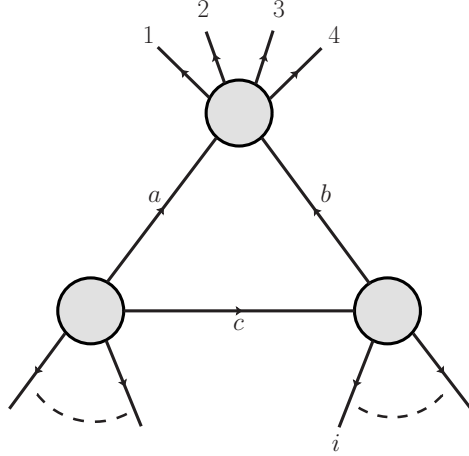


Figure 6: A one-loop cut diagram with a six-point tree-level amplitude at one corner.

participating tree amplitudes is a four-point amplitude. As we reviewed earlier, these particular supercoefficients can be obtained from certain associated BCFW tree-level diagrams, denoted as Y in the previous sections, and the precise correspondence is given in (2.17). Using this result, we can rewrite $\mathcal{C}_{n;1234;i}$ as

$$\begin{aligned} \mathcal{C}_{n;1234;i} &= -\frac{1}{4} \langle \hat{1} \hat{P} \rangle \langle \xi_{5i} \mu_{5i} \rangle \langle \xi_{i+1n} \mu_{i+1n} \rangle \left[\mathcal{M}(\bar{3}, 4, -\hat{\bar{P}}, \hat{2}) \circ (Y_{n-2;\hat{1}\hat{P};i}^{(1)} - Y_{n-2;\hat{1}\hat{P};i}^{(2)}) \right]_{z_1} \\ &+ (z_1 \leftrightarrow z_2), \end{aligned} \quad (4.4)$$

where a specific choice of signs has been made to rewrite massive momenta in terms of spinors (see (2.20)),

$$\sqrt{P_{5i}^2 P_{i+1n}^2} = -(1/4) \langle \xi_{5i} \mu_{5i} \rangle \langle \xi_{i+1n} \mu_{i+1n} \rangle. \quad (4.5)$$

In (4.4) we have also introduced a more informative notation for the Y -functions, in that we now specify the total number of legs ($n-2$ in the present case). This is because when repeatedly applying recursion relations, we have to deal with several Y -functions with different number of legs at the same time. For instance, the Y -function appearing in (4.4) is

$$Y_{n-2;\hat{1}\hat{P};i}^{(\alpha)} := \left[\mathcal{M}^{(0)}(\bar{5}, \dots, i, -\hat{\bar{P}}_{1P}, \hat{P}) \circ \mathcal{M}^{(0)}(\overline{i+1}, \dots, n, \hat{1}, \hat{P}_{1P}) \right]_{z_{\hat{1}\hat{P}}}, \quad (4.6)$$

with $\alpha = 1, 2$, and where \hat{P}_{1P} denotes the propagator of the BCFW diagram with legs $\hat{1}$, \hat{P} being shifted. We have also added a superscript to the pole solutions z_α – for instance $z_\alpha^{\hat{1}\hat{P}}$ refers to a recursive diagram with shifted legs $\hat{1}$ and \hat{P} .

We also find it convenient to introduce a more general notation $Y_{n;i i+1;k}^{(\alpha)}$ in order to capture the result of an iterated recursion. To this end we define the functions

$$Y_{n;i_1 i_2; i_2 i_3; \dots; i_{m_1} i_{m_2}; k_1; k_2; \dots; k_m}^{(\alpha_1; \alpha_2; \dots; \alpha_m)} \quad (4.7)$$

where n is again the total number of legs, and $i_{j_1} i_{j_2}$ indicate which adjacent pair of legs are shifted when we apply the j^{th} recursion relation. Finally, for each recursive diagram with shifts $i_{j_1} i_{j_2}$, we specify the corresponding channel by adding an index k_j , similarly to the index k in $Y_{n;i i+1;k}^{(\alpha)}$. The functions Y so defined appear in iterated BCFW recursions of tree amplitudes and are the natural building blocks of one-loop supercoefficients.

Making use of this more compact notation, we find⁹

$$\begin{aligned} Y_{n;12;\hat{1}\hat{P};4,i}^{(\alpha;\beta)} &:= \left[\mathcal{M}^{(0)}(\bar{3}, 4, -\bar{P}, \hat{2}) \circ Y_{n-2;\hat{1}\hat{P};i}^{(\beta)} \right]_{z_\alpha^{12}} \\ &= \left[\mathcal{M}^{(0)}(\bar{3}, 4, -\bar{P}, \hat{2}) \circ \left[\mathcal{M}^{(0)}(\bar{5}, \dots, i, -\bar{P}_{1P}, \hat{P}) \circ \mathcal{M}^{(0)}(\bar{i+1}, \dots, n, \hat{1}, \hat{P}_{1P}) \right]_{z_\beta^{\hat{1}\hat{P}}} \right]_{z_\alpha^{12}}. \end{aligned} \quad (4.8)$$

Thus we can rewrite the one-loop supercoefficient as

$$\mathcal{C}_{n;1234;i} = \frac{1}{4} \langle \xi_{5i} \mu_{5i} \rangle \langle \xi_{i+1n} \mu_{i+1n} \rangle \sum_{\alpha,\beta=1}^2 (-)^\beta \langle \hat{1} \hat{P} \rangle Y_{n;12;\hat{1}\hat{P};4,i}^{(\alpha;\beta)}. \quad (4.9)$$

It is easy to evaluate $\langle \hat{1} \hat{P} \rangle$ explicitly using the solution for $\lambda_{\hat{P}}$ in (A.3), with the result

$$\langle \hat{1} \hat{P} \rangle \Big|_{z_1^{12}} = \frac{i}{2} \langle \xi_{14} \mu_{14} \rangle, \quad \langle \hat{1} \hat{P} \rangle \Big|_{z_2^{12}} = -\frac{i}{2} \langle \xi_{14} \mu_{14} \rangle. \quad (4.10)$$

Using this, (4.9) becomes

$$\mathcal{C}_{n;1234;i} = \frac{i}{8} \langle \xi_{14} \mu_{14} \rangle \langle \xi_{5i} \mu_{5i} \rangle \langle \xi_{i+1n} \mu_{i+1n} \rangle \sum_{\alpha,\beta=1}^2 (-)^{\alpha+\beta+1} Y_{n;12;\hat{1}\hat{P};4,i}^{(\alpha;\beta)}. \quad (4.11)$$

Multiplying $\mathcal{C}_{n;1234;i}$ with the corresponding three-mass triangle we obtain the contribution of this diagram to the one-loop amplitude,

$$\mathcal{C}_{n;1234;i} \mathcal{I}_{1,4;5,i;i+1,n} = \mathcal{S}_{1,4;5,i;i+1,n} \sum_{\alpha,\beta=1}^2 (-)^{\alpha+\beta+1} Y_{n;12;\hat{1}\hat{P};4,i}^{(\alpha;\beta)}, \quad (4.12)$$

where the pre-factor $\mathcal{S}_{1,4;5,i;i+1,n}$ is¹⁰

$$\mathcal{S}_{1,4;5,i;i+1,n} = \frac{\pi^3}{8} \frac{\langle \xi_{14} \mu_{14} \rangle \langle \xi_{5i} \mu_{5i} \rangle \langle \xi_{i+1n} \mu_{i+1n} \rangle}{\sqrt{-(P_{1,4}^2 + i\varepsilon)} \sqrt{-(P_{5,i}^2 + i\varepsilon)} \sqrt{-(P_{i+1,n}^2 + i\varepsilon)}}. \quad (4.13)$$

⁹In order to perform this further shift on $\lambda_{\hat{P}}$ explicitly, one may use its explicit expression given in (A.3).

¹⁰For the sake of clarity, we remind the reader that $Y_{n;12;\hat{1}\hat{P};4,i}^{(\alpha;\beta)}$ is a tree recursive diagram which would appear in the tree-level amplitude $\mathcal{M}_n^{(0)}(\bar{1}, 2, \dots, n)$, namely $\sum_{\alpha,\beta=1}^2 Y_{n;12;\hat{1}\hat{P};4,i}^{(\alpha;\beta)} \in \mathcal{M}_n^{(0)}(\bar{1}, 2, \dots, n)$.

4.2 Eight-point amplitude at one corner

Before discussing the case of a generic one-loop supercoefficient, we consider a slightly more sophisticated example in detail, specifically the situation where a tree-level amplitude at one corner of the triple-cut diagram is an eight-point amplitude. Such a supercoefficient can be written as

$$\mathcal{C}_{n;1,\dots,6;i} = \frac{1}{2} \sum_{s=1}^2 \int d^3\eta_a d^3\eta_b d^3\eta_c \mathcal{M}^{(0)}(\bar{1}, \dots, 6, -\bar{b}_s, -a_s) \mathcal{M}^{(0)}(\bar{7}, \dots, i, -\bar{c}_s, b_s) \mathcal{M}^{(0)}(\bar{i+1}, \dots, n, \bar{a}_s, c_s). \quad (4.14)$$

We can derive this from a recursion relation with legs 1 and 2 shifted:

$$\begin{aligned} \mathcal{C}_{n;1,\dots,6;i} &= - \left[\mathcal{M}^{(0)}(\bar{3}, \dots, 6, -\bar{P}, \hat{2}) \circ \mathcal{C}_{n-4;\hat{1}\hat{P};i} \right]_{z_1^{12}} + \left[\mathcal{M}^{(0)}(\bar{3}, 4, -\bar{P}, \hat{2}) \circ \mathcal{C}_{n-2;\hat{1}\hat{P}56;i} \right]_{z_1^{12}} \\ &+ (z_1^{12} \leftrightarrow z_2^{12}). \end{aligned} \quad (4.15)$$

The first term on the right-hand side of (4.15) needs no further reduction as it already contains a supercoefficient which can be derived using the correspondence with tree-level recursive diagrams of [12]. On the other hand, for the second term we can apply once more the supercoefficient recursion relation, shifting for instance the legs 5 and 6 of $\mathcal{C}_{n-2;\hat{1}\hat{P}56;i}$. To distinguish the new shifts from those of the first recursion relation, we denote them as $\hat{5}'$, $\hat{6}'$, and the propagator in the corresponding recursive diagram as \hat{P}' . After applying this second recursion, $\mathcal{C}_{n;1,\dots,6;i}$ can be written as

$$\begin{aligned} \mathcal{C}_{n;1,\dots,6;i} &= - \left[\mathcal{M}^{(0)}(\bar{3}, \dots, 6, -\bar{P}, \hat{2}) \circ \mathcal{C}_{n-4;\hat{1}\hat{P};i} \right]_{z_1^{12}} \\ &+ \left[\left[\mathcal{M}^{(0)}(\bar{3}, 4, -\bar{P}, \hat{2}) \circ \left[\mathcal{M}^{(0)}(\bar{1}, \hat{P}, \bar{5}', \hat{P}') \circ (-\mathcal{C}_{n-4;-\hat{P}'\hat{6}';i}) \right]_{z_1^{56}} \right]_{z_1^{12}} \right. \\ &\left. + (z_1^{56} \leftrightarrow z_2^{56}) \right] + (z_1^{12} \leftrightarrow z_2^{12}) \\ &= - \left[\mathcal{M}^{(0)}(\bar{3}, \dots, 6, -\bar{P}, \hat{2}) \circ \mathcal{C}_{n-4;\hat{1}\hat{P};i} \right]_{z_1^{12}} \\ &+ \left[\mathcal{M}^{(0)}(\bar{1}, 2, \bar{3}, 4, \bar{5}', \hat{P}') \circ \mathcal{C}_{n-4;-\hat{P}'\hat{6}';i} \right]_{z_1^{56}} \\ &+ (z_1^{56} \leftrightarrow z_2^{56}) + (z_1^{12} \leftrightarrow z_2^{12}), \end{aligned} \quad (4.16)$$

where in the last step we used

$$\left[\mathcal{M}^{(0)}(\bar{3}, 4, -\bar{P}, \hat{2}) \circ \mathcal{M}^{(0)}(\bar{1}, \hat{P}, \bar{5}', \hat{P}') \right]_{z_1^{12}} + (z_1^{12} \leftrightarrow z_2^{12}) = -\mathcal{M}^{(0)}(\bar{1}, 2, \bar{3}, 4, \bar{5}', \hat{P}'). \quad (4.17)$$

Now we have reached the extremal case when all the supercoefficients have at least one corner with a four-point amplitude, so we are ready to apply the connection between these special triple-cuts and tree-level recursion relations, and find

$$\mathcal{C}_{n;1,\dots,6;i} = \frac{1}{4} \langle \xi_{7i} \mu_{7i} \rangle \langle \xi_{i+1n} \mu_{i+1n} \rangle$$

$$\begin{aligned}
& \times \left(- \langle \hat{1} \hat{P} \rangle [\mathcal{M}^{(0)}(\bar{3}, \dots, 6, -\bar{P}, \hat{2}) \circ (Y_{n-4; \hat{1} \hat{P}; i}^{(1)} - Y_{n-4; \hat{1} \hat{P}; i}^{(2)})]_{z_1^{12}} \right. \\
& \left. + i \langle \hat{P} \hat{6} \rangle [\mathcal{M}^{(0)}(\bar{1}, 2, \bar{3}, 4, \bar{5}, \hat{P}) \circ (Y_{n-4; -\hat{P} \hat{6}; i}^{(1)} - Y_{n-4; -\hat{P} \hat{6}; i}^{(2)})]_{z_1^{56}} \right) \\
& + (z_1^{56} \leftrightarrow z_2^{56}) + (z_1^{12} \leftrightarrow z_2^{12}), \tag{4.18}
\end{aligned}$$

where in the second line the prime on the shifted legs 5 and 6 has been removed, since in this expression we only perform BCFW shifts on legs 5 and 6, but not legs 1 and 2. Various terms in (4.18) can be combined into the Y -functions defined in (4.7). After some simple manipulations we obtain

$$\mathcal{C}_{n;1,\dots,6;i} = \frac{i}{8} \langle \xi_{16} \mu_{16} \rangle \langle \xi_{7i} \mu_{7i} \rangle \langle \xi_{i+1n} \mu_{i+1n} \rangle \sum_{\alpha, \beta=1}^2 (-)^{\alpha+\beta+1} (Y_{n;12; \hat{1} \hat{P}; 6; i}^{(\alpha; \beta)} + Y_{n;56; -\hat{P} \hat{6}; n; i}^{(\alpha; \beta)}), \tag{4.19}$$

where we have used the fact that $\langle \hat{1} \hat{P} \rangle$ and $i \langle \hat{P} \hat{6} \rangle$ can be written in terms of $\langle \xi_{16} \mu_{16} \rangle$. Multiplying $\mathcal{C}_{n;1,\dots,6;i}$ with the corresponding three-mass triangle integral, we obtain the one-loop contribution of this diagram,

$$\mathcal{C}_{n;1,\dots,6;i} I_{1,6;7,i;i+1,n} = \mathcal{S}_{1,6;7,i;i+1,n} \sum_{\alpha, \beta=1}^2 (-)^{\alpha+\beta+1} (Y_{n;12; \hat{1} \hat{P}; 6; i}^{(\alpha; \beta)} + Y_{n;56; -\hat{P} \hat{6}; n; i}^{(\alpha; \beta)}), \tag{4.20}$$

where the pre-factor $\mathcal{S}_{1,6;7,i;i+1,n}$ is

$$\mathcal{S}_{1,6;7,i;i+1,n} = \frac{\pi^3}{8} \frac{\langle \xi_{16} \mu_{16} \rangle \langle \xi_{7i} \mu_{7i} \rangle \langle \xi_{i+1n} \mu_{i+1n} \rangle}{\sqrt{-(P_{1,6}^2 + i\varepsilon)} \sqrt{-(P_{7,i}^2 + i\varepsilon)} \sqrt{-(P_{i+1,n}^2 + i\varepsilon)}}. \tag{4.21}$$

4.3 The general one-loop supercoefficients

It is not difficult to generalise the results of the previous subsections to arbitrary supercoefficients such as (3.1). Without loss of generality we focus on the tree-level amplitude $\mathcal{M}^{(0)}(\bar{1}, \dots, m, -\bar{b}, -a)$. The idea is to repeatedly apply the recursion relation in order to reduce it to a four-point amplitude, and then apply the connection between anomalous triple cuts and tree-level recursion diagrams.

As in the special cases of the previous subsections, we start by shifting legs 1 and 2, followed by shifts of legs $m-1$ and m . After that, we shift the two left-most legs of that corner, namely the shifted leg 1 and the corresponding shifted propagator. Generally we denote them as $\hat{1}_q$ and \hat{P}_q , *i.e.* we call them as $\hat{1}_1$ and \hat{P}_1 when they are shifted in the first iteration, and $\hat{1}_2$ and \hat{P}_2 in the second iteration, and so on. This process terminates whenever we reach the extremal case, namely when an $(m+2)$ -point amplitude at the corner reduces to a four-point amplitude. The result of this procedure is

$$\mathcal{C}_{n;1,2,\dots,m;i} = \frac{i}{8} \langle \xi_{1m} \mu_{1m} \rangle \langle \xi_{m+1i} \mu_{m+1i} \rangle \langle \xi_{i+1n} \mu_{i+1n} \rangle \tag{4.22}$$

$$\begin{aligned}
& \times \left(\sum_{\alpha, \beta=1}^2 (-)^{\alpha+\beta+1} (Y_{n;1\,2;1_1\,P_1;m;i}^{(\alpha;\beta)} + Y_{n;m-1\,m;-P_1\,m_1;n;i}^{(\alpha;\beta)}) \right. \\
& \left. + \sum_{j, \alpha, k} (-)^{\frac{k_1+\dots+k_{j-1}}{2} + \frac{m(j+1)}{2} + \alpha_0 + \alpha_{j+1}} Y_{n;12;1_1 P_1; \dots; 1_{j+1} P_{j+1}; k_0; k_1; \dots; k_{j-1}; m; i}^{(\alpha_0; \alpha_1; \dots; \alpha_{j+1})} \right),
\end{aligned}$$

where the summation in the last term is over j , the α 's, which can be 1 and 2, and all the k 's, which must be even with $k_p < k_q$ if $p < q$. In order to arrive at the expression in the last line of (4.22) we used the following identity

$$\begin{aligned}
& \left[\mathcal{M}^{(0)}(\overline{k_j+1}, \dots, k_f, -\widehat{P}_{m-1, m}, \widehat{m}) \circ \mathcal{M}^{(0)}(\overline{k_f+1}, \dots, \widehat{m-1}, \widehat{P}_{m-1, m}) \right]_{z_1} + (z_1 \leftrightarrow z_2) \\
& = \mathcal{M}^{(0)}(\overline{m-1}, m, \widehat{P}_{1_j P_j}, \widehat{P}_j, \overline{k_j+1}, \dots, k_f, \overline{k_f+1}, \dots, m-2) \\
& = \mathcal{M}^{(0)}(\overline{k_j+1}, \dots, k_f, \overline{k_f+1}, \dots, m-2, \overline{m-1}, m, \widehat{P}_{1_j P_j}, \widehat{P}_j). \tag{4.23}
\end{aligned}$$

To obtain the contribution to the one-loop amplitude we simply multiply the supercoefficient with the corresponding triangle integral, with the result

$$\begin{aligned}
& \mathcal{C}_{n;1,2,\dots,m;i} \mathcal{I}_{1,m;m+1,i;j+1,n} = \mathcal{S}_{1,m;m+1,i;j+1,n} \\
& \times \left[\sum_{\alpha, \beta=1}^2 (-)^{\alpha+\beta+1} (Y_{n;1\,2;1_1\,P_1;m;i}^{(\alpha;\beta)} + Y_{n;m-1\,m;-P_1\,m_1;n;i}^{(\alpha;\beta)}) \right. \\
& \left. + \sum_{j, \alpha, k} (-)^{\frac{k_1+\dots+k_{j-1}}{2} + \frac{m(j+1)}{2} + \alpha_0 + \alpha_{j+1}} Y_{n;12;1_1 P_1; \dots; 1_{j+1} P_{j+1}; k_0; k_1; \dots; k_{j-1}; m; i}^{(\alpha_0; \alpha_1; \dots; \alpha_{j+1})} \right], \tag{4.24}
\end{aligned}$$

where

$$\mathcal{S}_{1,m;m+1,i;j+1,n} = \frac{\pi^3}{8} \frac{\langle \xi_{1m} \mu_{1m} \rangle \langle \xi_{m+1i} \mu_{m+1i} \rangle \langle \xi_{i+1n} \mu_{i+1n} \rangle}{\sqrt{-(P_{1,m}^2 + i\varepsilon)} \sqrt{-(P_{m+1,i}^2 + i\varepsilon)} \sqrt{-(P_{i+1,n}^2 + i\varepsilon)}}. \tag{4.25}$$

We wish to emphasise that by definition each sum of Y -functions (without the minus signs) in (4.24) is equal to terms which would appear in iterated BCFW recursion relations for tree amplitudes. In this sense, all one-loop amplitudes can be written as sums of tree-level recursive diagrams with possible minus signs. We also note that each term in this sum is dual conformal invariant.

Acknowledgements

We would like to thank Niklas Beisert, Paul Heslop, Valya Khoze and Bill Spence for stimulating discussions. This work was supported by the STFC Grant ST/J000469/1, ‘‘String theory, gauge theory & duality’’. AB thanks the Physics Departments at the Weizmann Institute of Science and Tel Aviv University for their hospitality. GT acknowledges the warm hospitality and support from the Institute for Particle Physics Phenomenology, Durham University, through an IPPP Associateship. We would also like to thank the ECT*, Trento, for hospitality and partial support.

A On-shell solution

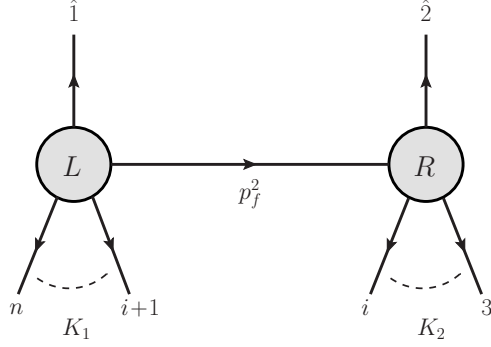


Figure 7: A BCFW recursive diagram of a tree-level amplitude. Here $K_1 = p_{i+1} + \dots + p_n$ and $K_2 = p_3 + \dots + p_i$.

We present here a solution for the spinor $\lambda_{\hat{P}}$ that appeared in the the BCFW recursion relations. In general, any two-dimensional vector can be expanded in terms of two independent vectors. In our case it is convenient to expand $\lambda_{\hat{P}}$ in terms of $\lambda_{\hat{1}}$ and $\lambda_{\hat{2}}$, as

$$\lambda_{\hat{P}} = \frac{1}{\langle \hat{1} \hat{2} \rangle} \left(\langle \hat{P} \hat{2} \rangle \lambda_{\hat{1}} + \langle \hat{1} \hat{P} \rangle \lambda_{\hat{2}} \right), \quad (\text{A.1})$$

where we have used that $\langle \hat{1} \hat{2} \rangle = \langle 1 2 \rangle$. (A.1) can be further simplified by applying momentum conservation, see Figure 7,

$$\begin{aligned} \langle \hat{P} \hat{1} \rangle^2 &= (\hat{P} + \hat{1})^2 = K_1^2 = -\frac{1}{4} \langle \xi_{i+1n} \mu_{i+1n} \rangle^2, \\ \langle \hat{P} \hat{2} \rangle^2 &= -(\hat{P} - \hat{2})^2 = -K_2^2 = \frac{1}{4} \langle \xi_{3i} \mu_{3i} \rangle^2, \end{aligned} \quad (\text{A.2})$$

where we have rewritten massive momenta in terms of spinors. Thus we arrive at the result

$$\lambda_{\hat{P}} = \pm \frac{1}{2\langle \hat{1} \hat{2} \rangle} \left(\langle \xi_{3i} \mu_{3i} \rangle \lambda_{\hat{1}} \pm i \langle \xi_{i+1n} \mu_{i+1n} \rangle \lambda_{\hat{2}} \right), \quad (\text{A.3})$$

where the four possible choices of signs correspond to the four possible BCFW on-shell solutions,

$$z_1^2 = \frac{\langle \xi_{i+1n} \mu_{3i} \rangle \langle \mu_{i+1n} \xi_{3i} \rangle}{\langle \lambda_1 + i\lambda_2 | K_1 | \lambda_1 + i\lambda_2 \rangle}, \quad z_2^2 = \frac{\langle \xi_{i+1n} \xi_{3i} \rangle \langle \mu_{i+1n} \mu_{3i} \rangle}{\langle \lambda_1 + i\lambda_2 | K_1 | \lambda_1 + i\lambda_2 \rangle}. \quad (\text{A.4})$$

References

- [1] O. Aharony, O. Bergman, D. L. Jafferis and J. Maldacena, *N=6 superconformal Chern-Simons-matter theories, M2-branes and their gravity duals*, JHEP **0810** (2008) 091 [arXiv:0806.1218 [hep-th]].
- [2] J. A. Minahan, K. Zarembo, *The Bethe ansatz for superconformal Chern-Simons*, JHEP **0809** (2008) 040, [arXiv:0806.3951 [hep-th]];
- [3] J. A. Minahan, W. Schulgin, K. Zarembo, *Two loop integrability for Chern-Simons theories with N=6 supersymmetry*, JHEP **0903** (2009) 057, [arXiv:0901.1142 [hep-th]].
- [4] G. Arutyunov and S. Frolov, *Superstrings on AdS(4) x CP**3 as a Coset Sigma-model*, JHEP **0809** (2008) 129 [arXiv:0806.4940 [hep-th]].
- [5] B. Stefanski, jr, *Green-Schwarz action for Type IIA strings on AdS(4) x CP**3*, Nucl. Phys. B **808** (2009) 80 [arXiv:0806.4948 [hep-th]].
- [6] D. Sorokin and L. Wulff, *Evidence for the classical integrability of the complete AdS4xCP3 superstring*, JHEP **1011** (2010) 143 [arXiv:1009.3498 [hep-th]].
- [7] T. Bargheer, F. Loebbert and C. Meneghelli, *Symmetries of Tree-level Scattering Amplitudes in N=6 Superconformal Chern-Simons Theory*, Phys. Rev. D **82** (2010) 045016 [arXiv:1003.6120 [hep-th]].
- [8] Y. -t. Huang and A. E. Lipstein, *Dual Superconformal Symmetry of N=6 Chern-Simons Theory*, JHEP **1011** (2010) 076 [arXiv:1008.0041 [hep-th]].
- [9] D. Gang, Y. -t. Huang, E. Koh, S. Lee and A. E. Lipstein, *Tree-level Recursion Relation and Dual Superconformal Symmetry of the ABJM Theory*, JHEP **1103** (2011) 116 [arXiv:1012.5032 [hep-th]].
- [10] W. -M. Chen and Y. -t. Huang, *Dualities for Loop Amplitudes of N=6 Chern-Simons Matter Theory*, JHEP **1111** (2011) 057 [arXiv:1107.2710 [hep-th]].
- [11] T. Bargheer, N. Beisert, F. Loebbert and T. McLoughlin, *Conformal Anomaly for Amplitudes in N=6 Superconformal Chern-Simons Theory*, arXiv:1204.4406 [hep-th].
- [12] A. Brandhuber, G. Travaglini and C. Wen, *A note on amplitudes in N=6 superconformal Chern-Simons theory*, arXiv:1205.6705 [hep-th], to appear in JHEP.
- [13] S. Lee, *Yangian Invariant Scattering Amplitudes in Supersymmetric Chern-Simons Theory*, Phys. Rev. Lett. **105** (2010) 151603 [arXiv:1007.4772 [hep-th]].
- [14] M. S. Bianchi, M. Leoni, A. Mauri, S. Penati and A. Santambrogio, *One Loop Amplitudes In ABJM*, arXiv:1204.4407 [hep-th].
- [15] Y. -t. Huang and S. Lee, *A new integral formula for supersymmetric scattering amplitudes in three dimensions*, arXiv:1207.4851 [hep-th].

- [16] A. Agarwal, N. Beisert and T. McLoughlin, *Scattering in Mass-Deformed $N \geq 4$ Chern-Simons Models*, JHEP **0906** (2009) 045 [arXiv:0812.3367 [hep-th]].
- [17] A. Lipstein and L. Mason, *Amplitudes of 3d Yang-Mills theory*, [arXiv:1207.6176 [hep-th]].
- [18] Y. -t. Huang, seminar given at the workshop “Recent Advances in Scattering Amplitudes”, Newton Institute for Mathematical Sciences, Cambridge, 4th April 2012, <http://www.newton.ac.uk/programmes/BSM/seminars/040409001.html>
- [19] R. Roiban, M. Spradlin and A. Volovich, *Dissolving $N=4$ loop amplitudes into QCD tree amplitudes*, Phys. Rev. Lett. **94** (2005) 102002 [hep-th/0412265].
- [20] M. S. Bianchi, M. Leoni, A. Mauri, S. Penati and A. Santambrogio, *Scattering Amplitudes/Wilson Loop Duality In ABJM Theory*, JHEP **1201** (2012) 056 [arXiv:1107.3139 [hep-th]].
- [21] M. S. Bianchi, M. Leoni and S. Penati, *An All Order Identity between ABJM and $N=4$ SYM Four-Point Amplitudes*, JHEP **1204** (2012) 045 [arXiv:1112.3649 [hep-th]].
- [22] L. F. Alday and J. M. Maldacena, *Gluon scattering amplitudes at strong coupling*, JHEP **0706**, 064 (2007), [arXiv:0705.0303 [hep-th]].
- [23] J. M. Drummond, G. P. Korchemsky and E. Sokatchev, *Conformal properties of four-gluon planar amplitudes and Wilson loops*, Nucl. Phys. B **795**, 385 (2008), [arXiv:0707.0243 [hep-th]].
- [24] A. Brandhuber, P. Heslop and G. Travaglini, *MHV amplitudes in $N=4$ super Yang-Mills and Wilson loops*, Nucl. Phys. B **794**, 231 (2008), [arXiv:0707.1153 [hep-th]].
- [25] J. M. Henn, J. Plefka and K. Wiegandt, *Light-like polygonal Wilson loops in 3d Chern-Simons and ABJM theory*, JHEP **1008** (2010) 032 [Erratum-ibid. **1111** (2011) 053] [arXiv:1004.0226 [hep-th]].
- [26] M. S. Bianchi, M. Leoni, A. Mauri, S. Penati, C. A. Ratti and A. Santambrogio, *From Correlators to Wilson Loops in Chern-Simons Matter Theories*, JHEP **1106** (2011) 118 [arXiv:1103.3675 [hep-th]].
- [27] K. Wiegandt, *Equivalence of Wilson Loops in $\mathcal{N} = 6$ super Chern-Simons matter theory and $\mathcal{N} = 4$ SYM Theory*, Phys. Rev. D **84** (2011) 126015 [arXiv:1110.1373 [hep-th]].
- [28] Z. Bern and G. Chalmers, *Factorization in one loop gauge theory*, Nucl. Phys. B **447** (1995) 465 [hep-ph/9503236].
- [29] Z. Bern, N. E. J. Bjerrum-Bohr, D. C. Dunbar and H. Ita, *Recursive calculation of one-loop QCD integral coefficients*, JHEP **0511**, 027 (2005) [hep-ph/0507019].